

## RESEARCH ARTICLE

## Bioseparations and Downstream Processing

# New technical concept for alternating tangential flow filtration in biotechnological cell separation processes

Maria E. Weinberger  | Luis Schoch | Ulrich Kulozik

Technical University of Munich, TUM School of Life Sciences, Chair of Food and Bioprocess Engineering, Freising, Germany

**Correspondence**

Maria E. Weinberger, Technical University of Munich, TUM School of Life Sciences, Chair of Food and Bioprocess Engineering, Weihenstephaner Berg 1, 85354 Freising, Germany.  
Email: [maria.weinberger@tum.de](mailto:maria.weinberger@tum.de)

**Abstract**

Robust cell retention devices are key to successful cell culture perfusion. Currently, tangential flow filtration (TFF) and alternating tangential flow filtration (ATF) are most commonly used for this purpose. TFF, however, suffers from poor fouling mitigation, which leads to high filtration resistance and product retention, and ATF suffers from long residence times and cell accumulation. In this work, we propose a filtration system for alternating tangential flow filtration, which takes full advantage of the fouling mitigation effects of alternating flow and reduces cell accumulation. We have tested this novel setup in direct comparison with the XCell ATF<sup>®</sup> as well as TFF with a model feed comprising yeast cells and bovine serum albumin as protein at harsh permeate to feed flow conditions. We found that by avoiding the dead-end design of a diaphragm pump, the proposed filtration system exhibited a reduced filtration resistance by approximately 20% to 30% (depending on feed rate and permeate flow rate). A further improvement of the novel setup was reached by optimization of phase durations and flow control, which resulted in a fourfold extension of process duration until hollow fiber flow channel blockage occurred. Thus, the proposed concept appears to be superior to current cell retention devices in perfusion technology.

**KEYWORDS**

cell retention, crossflow filtration, deposit formation, low-shear, microfiltration, product sieving

## 1 | INTRODUCTION

Perfusion processes have gained in importance in biopharmaceutical cellular fermentation processes and research alike during the last few decades<sup>1,2</sup> due to increased productivity, improved product quality and higher batch-to-batch homogeneity in comparison to fed-batch processes.<sup>3,4</sup> The critical point is generally seen in the perfusion or cell retention device,<sup>5,6</sup> which is designed for separating the produced biological therapeutic substance in continuous production mode over longer periods of processing time, while retaining the producing cells. Among the membrane-based perfusion devices, conventional tangential

flow filtration (TFF) and alternating tangential flow filtration (ATF), that is, crossflow with periodically changing flow direction, are commonly used. In membrane-based perfusion processes, a key process performance indicator is the transmission of the target molecule (also known as product sieving). Deposits formed by retained cells and macromolecules can add an additional retention effect in comparison to the clean membrane. This deposit formation often results in reduced transmission, as it acts as a secondary membrane with its own and often unpredictable retention characteristics. Published work shows the superiority of ATF over TFF in terms of higher cell viability and lower product retention.<sup>7,8</sup> The ATF concept has become widely applied in the

This is an open access article under the terms of the [Creative Commons Attribution](https://creativecommons.org/licenses/by/4.0/) License, which permits use, distribution and reproduction in any medium, provided the original work is properly cited.

© 2022 The Authors. *Biotechnology Progress* published by Wiley Periodicals LLC on behalf of American Institute of Chemical Engineers.

biopharmaceutical industry through the development of the commercially available XCell ATF<sup>®</sup> device. Besides its application as perfusion device in the production of monoclonal antibodies,<sup>8,9</sup> it has also been studied for the production of virus particles,<sup>10</sup> to intensify N-1 seeding fermentation<sup>11</sup> and for harvesting of biopharmaceuticals.<sup>12</sup>

The superior performance of the XCell ATF<sup>®</sup> device versus conventional TFF has been attributed to three main effects: Firstly, the feed pump used in this system, a diaphragm pump, is considered a low-shear pump. The use of low-shear pumps was reported to result in low cell damage and therefore a lower release of DNA, RNA and other intracellular substances into the fermentation broth.<sup>13</sup> This reduces the complexity of substances in the aqueous phase, thus reducing fouling propensity, which otherwise increase filtration resistance and product retention. Secondly, these fouling effects were reported to be under better control by flow reversal and the associated pressure pulsations, which promote fouling mitigation and thus enhance filtration performance.<sup>14</sup> Thirdly, the changing pressure conditions of the unsteady flow were reported to cause backflushing of filtrate back to the retentate, also described as Starling flow phenomena,<sup>15</sup> which contributes to the removal of deposited material from the membrane surface. The fouling mitigation effects of alternating crossflow<sup>14,16–18</sup> and other hydrodynamic fouling mitigation techniques have been extensively described in several works.<sup>19–21</sup>

The remaining critical point, though, in our eyes is that the diaphragm pump applied in the XCell ATF<sup>®</sup> device is limited in its operational flexibility, long-term processing and technically feasible range of processing conditions. Also, scaling up beyond XCell ATF<sup>®</sup> 10, the largest commercially available device, is currently only possible by operating multiple units in parallel. The diaphragm pump is pneumatically actuated by supplying pressurized air and vacuum from the reverse side of the diaphragm, which results in a flow from the diaphragm pump back to the feed vessel (pressure phase) and from the feed vessel to the diaphragm pump (exhaust phase), respectively.<sup>22</sup> The use of pressurized air and vacuum, however, leads to small achievable flow velocities, for instance a maximum of 10 L min<sup>-1</sup> in an XCell ATF<sup>®</sup> 4 device, which results in a crossflow velocity of only 0.25 m s<sup>-1</sup> in the attached hollow fiber module. Therefore, the wall shear stress along the membrane or deposit surface is limited to levels where only marginal deposit removal and fouling mitigation occurs. In perfusion processes of shear sensitive cells or mycelium-like aggregates, low crossflow velocities are well justified or even preferred, but for other processes working with more robust cells like yeasts, for instance *Pichia pastoris*, higher crossflow velocities could be desirable to enhance deposit layer removal. Several patents propose the advancement of the XCell ATF<sup>®</sup> device by employing two diaphragms instead of one, motorized actuators, pistons or combinations thereof.<sup>23–25</sup> However, these technical developments appear to be mechanically complex to implement and they are not commercially available so far.

Another important aspect is that the diaphragm pump volume limits the pump's maximum displacement volume per stroke and cycle. Therefore, the duration of each forward and backward cycle of alternating flow depends on the targeted flow rate. This interdependence limits the options for process optimization, as both frequency and

crossflow velocity have an impact on the extent of fouling and fouling mitigation.<sup>16,26</sup> If, for instance, the crossflow velocity is reduced in order to decrease the shear stress acting on the cells, also the frequency will be reduced, which may have a negative impact on effective fouling mitigation. Additionally, the ratio of hold-up volume in the transfer line to the bioreactor and filter module relative to the fixed pump displacement volume can also be seen as unfavorable. This is because it provokes long residence times of cells in the device, which can lead to oxygen depletion, increased lactate production and reduced growth rate, impaired viability, and lower productivity.<sup>27,28</sup> Under certain processing conditions, cells even accumulate in the diaphragm hold-up volume, which leads to increased fluid viscosities and intensification of all aforementioned disadvantages, which are residence time related. That is why another patent proposes to replace the diaphragm pump with a bidirectional peristaltic pump.<sup>28</sup> The use of a peristaltic pump to transport the cell broth, however, poses an unwanted shear stress on the cells and is therefore not optimal for mammalian cell perfusion cultures.

Considering the reported advantages of alternating tangential flow filtration and to overcome the issues described above, a mechanically simple and more versatile alternating flow setup, capable of generating alternating flow within a wide range of flow rates and flow reversal frequencies would be desirable. At the same time, only low shear stress on the cells should be applied, residence times outside the bioreactor should be reduced and accumulation of cells in the external loop should be avoided. Therefore, a newly developed alternative alternating flow concept, mainly based on applying another pump concept with rapidly reacting centrifugal pumps acting in opposite flow direction (denominated setup II in the following), was studied in this work and compared with the XCell ATF<sup>®</sup> device (setup I in the following). The detailed technical features of the used pumps are described in detail in the methods section.

The focus of this work was on the hydrodynamic conditions, that is, flow rates, pressure conditions, filtration resistances and cell accumulation effects of both filtration setups. A practicable model feed system was designed comprising yeast cells as a representative of producing cells and bovine serum albumin (BSA) as a substitute for produced biological substances meant to pass through the membrane. The application to a cell culture perfusion process must be the ultimate goal when developing new cell retention devices. At this stage of the work, the focus was on the hydrodynamic characterization of the proposed concept. However, the low-shear design of the pumps employed in setup II were already reported to have no significant damaging effect on mammalian cells.<sup>13</sup> The next step following this work therefore is the transfer of this concept to a mammalian perfusion culture and assessing the impact on cell viability, including cell size and cell metabolism, as well as product sieving and product quality.

Filtration experiments were conducted at different flow conditions in both setups in constant concentration mode by recycling the permeate back to the feed tank. Setup II was at first operated within the range of the process conditions feasible with setup I to allow a direct comparison of both. However, setup II has a wider range of possible process conditions, which allows optimization to overcome the aforementioned

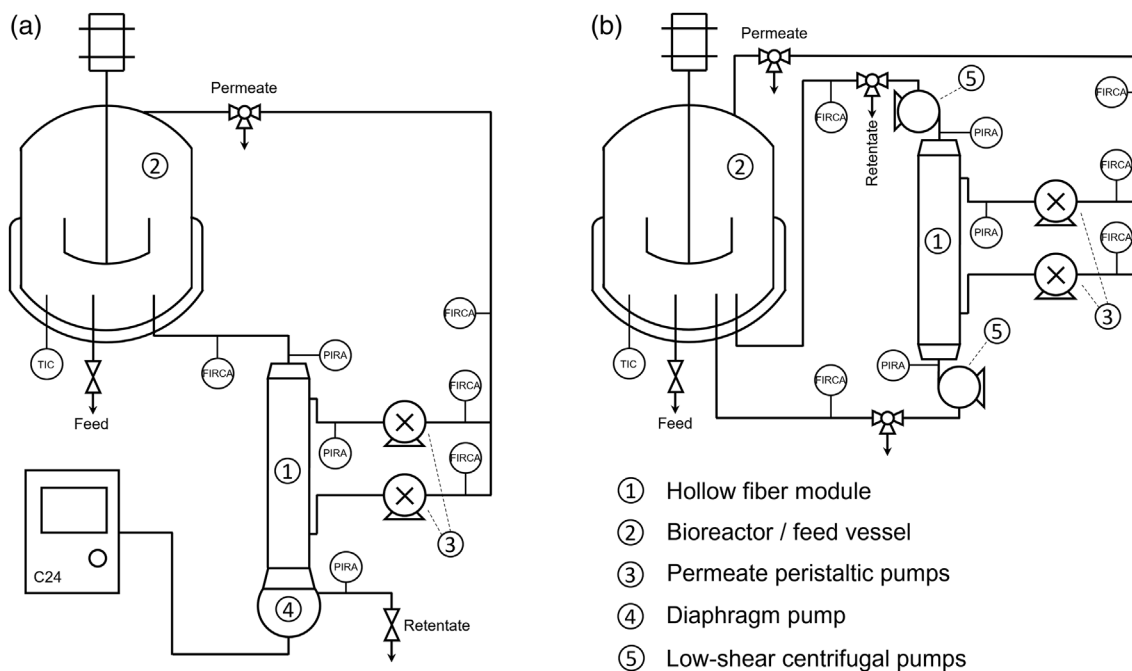


**FIGURE 1** Simplified P&I diagrams of the two different filtration setups comprising an XCell ATF<sup>®</sup> 4 device (setup I—panel A) or two counteractive centrifugal pumps with magnetically levitating impellers (setup II—panel B) for generation of alternating flow conditions.

cell accumulation issues. The permeate rates were intentionally chosen high in order to provoke the emergence of fouling and cell accumulation phenomena<sup>29</sup> for a better differentiation of both technical setups. Setup II was then further optimized under conditions outside the limitations of setup I. Inline data acquisition of flow velocities and pressures as well as regular sampling at different sampling points in the filtration systems combined with offline-analysis serve as data basis to evaluate filtration performance and process robustness.

## 2 | MATERIALS AND METHODS

### 2.1 | Filtration solution

The model feed used for all filtration trials was composed of yeast cells from the species *Saccharomyces cerevisiae* and BSA. The model feed was freshly prepared before each filtration trial by adding 0.8 g L<sup>-1</sup> of pre-dissolved BSA (Sigma Aldrich, St. Louis, Missouri, USA) and 150 g L<sup>-1</sup> unwashed fresh baker's yeast (F.X. Wieninger GmbH, Passau, Germany) to desalted water. The dry matter content of the feed solution was 4.3 ± 0.1% and the pH was 5.6 ± 0.2, with minor variations due to batch-to-batch variations of the fresh baker's yeast.

### 2.2 | Analytical methods

The dry matter content of feed and retentate samples was determined by a microwave assisted drying balance SMART 6 (CEM Corporation,

Matthews, North Carolina, USA). The dry matter content in the permeate was between 0.0 and 0.1% due to transmission of BSA and other solutes. As all permeate samples were clear and not turbid, transmission of cells could be excluded. The BSA contents in feed, retentate and permeate samples were determined by RP-HPLC according to Weinberger and Kulozik.<sup>26</sup> Transmission of BSA was calculated according to Equation (1) as the ratio of BSA contents in the permeate and in the feed.

$$Tr_{BSA} = \frac{c_{BSA,Permeate}}{c_{BSA,Feed}} \cdot 100\%. \quad (1)$$

### 2.3 | Filtration system

All filtration trials were conducted employing either of the two different filtration systems capable of generating alternating flow (see Figure 1 for a simplified P&I diagram of both setups). Setup I uses an XCell ATF<sup>®</sup> 4 device (Repligen Corporation, Waltham, Massachusetts, USA). The alternating flow in this setup is generated by a diaphragm pump, which is placed at the retentate side at the bottom end of the filter module. The diaphragm itself is driven by compressed air and vacuum, which is controlled by an ATF C24U v2.0 controller. The pump volume transported per stroke is 400 ml. The hold-up volume of the filtration module and the connecting tubing was approximately 260 ml. When the diaphragm moves downwards during the exhaust phase, fresh feed is drawn into the filtration module. When the diaphragm moves upwards during the pressure phase, the displaced volume is pushed back into the feed tank. The pump displacement

volume inextricably links the feed flow velocity generated by the XCell ATF<sup>®</sup> device to the cycle time of each forward and backwards phase. The XCell ATF<sup>®</sup> 4 supports feed flow volume throughputs between 1 and 10 L min<sup>-1</sup>.

Setup II uses two counteractive centrifugal pumps, type PuraLev<sup>®</sup> i100SU (Levitronix GmbH, Zurich, Switzerland), controlled by a console LCO-i100 (Levitronix GmbH, Zurich, Switzerland) to generate alternating flow directions. The impeller of these pumps are magnetically driven and actively magnetically levitated. Thus, narrow gaps are avoided, which would lead to high shear forces acting on the cells. This is why these pumps have been reported to be applicable even for shear sensitive mammalian cell perfusion cultures.<sup>13</sup> One of the pumps was positioned at each side of the filter module and the direction of flow was toward the module for both pumps. When the pump at the module inlet (which is defined as the bottom end of the module) was active and the feed flows forward, the second pump at the module outlet (top end of the module) was inactive and therefore the retentate flows through the inactive pump without significant resistance to flow. The pressure loss over the inactive pump can be neglected due to the bearingless design of the centrifugal pump. At the end of the forward phase, the bottom pump was set inactive and the top pump to active mode, which led to a flow reversal. Due to their bearingless design, the pumps can rapidly start up and shut down, which results in a sharp, almost step-wise flow profile. The pumps can also withstand the hydrodynamic stress posed by the frequent changes in flow velocity and direction. The maximum flow velocity in the given setup was 14 L min<sup>-1</sup> in either direction. The duration of forward and backward phases can be chosen independently from the flow velocity.

Except for the pumps generating the alternating flow, the two setups had the same main components. A temperature-controlled stirred tank bioreactor Biostat Cplus with 15 L maximum working volume (Sartorius AG, Goettingen, Germany), was used to provide the filtration fluid.

The filter module (F4:RF05PES, Repligen Corporation, Waltham, Massachusetts, USA) used was 35.8 cm long (with an effective fiber length of 29.5 cm). It comprised 830 hollow fibers made from polyether sulfone (PES) with an internal diameter of 1 mm, an effective membrane area of 0.77 m<sup>2</sup> and a retentate void volume of 234 ml. The membrane's nominal pore size was 0.5 μm.

The permeate was drawn by a dual head peristaltic pump (Heidolph Pumpdrive 5001, Heidolph Instruments GmbH & Co. KG, Kelheim, Germany) and was recycled to the feed tank. Feed, retentate and permeate lines were equipped with pressure sensors (PendoTECH, Princeton, New Jersey, USA). The permeate flow was measured with an ultrasonic high-precision flowmeter LFS-03SU-Z-SC1 (Levitronix GmbH, Zurich, Switzerland) and the feed flow with an ultrasonic clamp-on flowmeter LFSC-i16X (Levitronix GmbH, Zurich, Switzerland), which features a precise measurement in both flow directions. The retentate line of setup II was equipped with an additional ultrasonic clamp-on flowmeter LFSC-12D. In both setups, all sensors were connected to the console LCO-i100. The online data were collected with the Levitronix Service Software V2.0.7.3 (Levitronix GmbH, Zurich, Switzerland) with one data point per second. In preliminary experiments for flow profile characterization of

setup I and its reproduction in setup II (see Sections 2.4 and 3.1), the feed flow was logged with a LabVIEW application in order to retrieve high-resolution data with approximately 60 data points per second.

## 2.4 | Flow profile characterization

As a first step for comparing setups I and II, the flow profiles generated by setup I were recorded for several flow rates and reproduced with setup II. For this purpose, the bioreactor was filled with desalted water and kept at the filtration temperature of 15°C. The permeate line was closed throughout these preliminary tests. The feed rate was set on the ATF controller, which finds the right pre-pressure and orifice size in an iterative process. When the set feed rate was reached and the pre-pressure did not further change over time, the flow profile was recorded. It should be noted that it can take several minutes for the ATF controller to reach the flow set point. Therefore, the related pre-pressures and orifice sizes were recorded to be used as starting point in the following filtration experiments. Flow rates higher than 5 L min<sup>-1</sup> could not be sustained in setup I.

The flow profiles were analyzed in JMP<sup>®</sup> Pro 14.1 software and the actual flow in each phase and the phase duration were noted. These values were then used to program two-phase recipes on the console to set the duration of each phase and pump speed of the corresponding pump as input parameters for setup II.

## 2.5 | Filtration trial and data handling

Filtration experiments were conducted with both setups presented in Figure 1. Feed flow rate and permeate flow rate were varied independently in order to gain insights on the impact of crossflow velocity, flux and the ratio of permeate to feed flow on filtration performance. The permeate to feed ratio is reported to have an impact on the extent of backflushing<sup>15</sup> and thus on process performance. It is usually set to a value of 1:200 for perfusion processes and to a value of 1:20 for concentration processes.<sup>12</sup> However, harsh conditions up to a ratio of 1:3 were chosen in previous studies in order to provoke faster and more obvious fouling rates.<sup>29</sup> The chosen set point feed and permeate flow conditions of setup I are given in Table 1. It should be noted that the measured flow rates deviate from the set flow rates due to the indirect controlling strategy of the ATF controller, measuring cycle times instead of flow rates. The flow rates of setup II were set in order to match the actual flow rates of setup I, as can be seen from Figure 2. Shear rates  $\tau_w$  were calculated according to Equation (2) as a function of crossflow velocity  $v_{\text{crossflow}}$  and hollow fiber inner diameter  $d_i$ .

$$\tau_w = \frac{v_{\text{crossflow}} \cdot 8}{d_i} \quad (2)$$

Additionally to the experiments presented in Table 1, single experiments with forward flow only (i.e., conventional non-alternating

**TABLE 1** Overview over filtration trial set points in setup I. The set points of setup II were chosen to match the flow rates of setup I (see Figure 2)

Feed flow rate, L min <sup>-1</sup>	Crossflow velocity, <sup>a</sup> m s <sup>-1</sup>	Shear rate, s <sup>-1</sup>	Permeate flow rate, ml min <sup>-1</sup>	Flux, <sup>a</sup> L m <sup>-2</sup> h <sup>-1</sup>	Permeate to feed ratio
2	0.05	409	200	15.6	1:10
2	0.05	409	400	31.3	1:5
4	0.10	818	200	15.6	1:20
4	0.10	818	400	31.3	1:10

<sup>a</sup>Note that crossflow velocity and flux can be calculated from feed and permeate flow rate by considering the membrane geometry. These values are given here in order to facilitate a direct comparison with data from other studies.

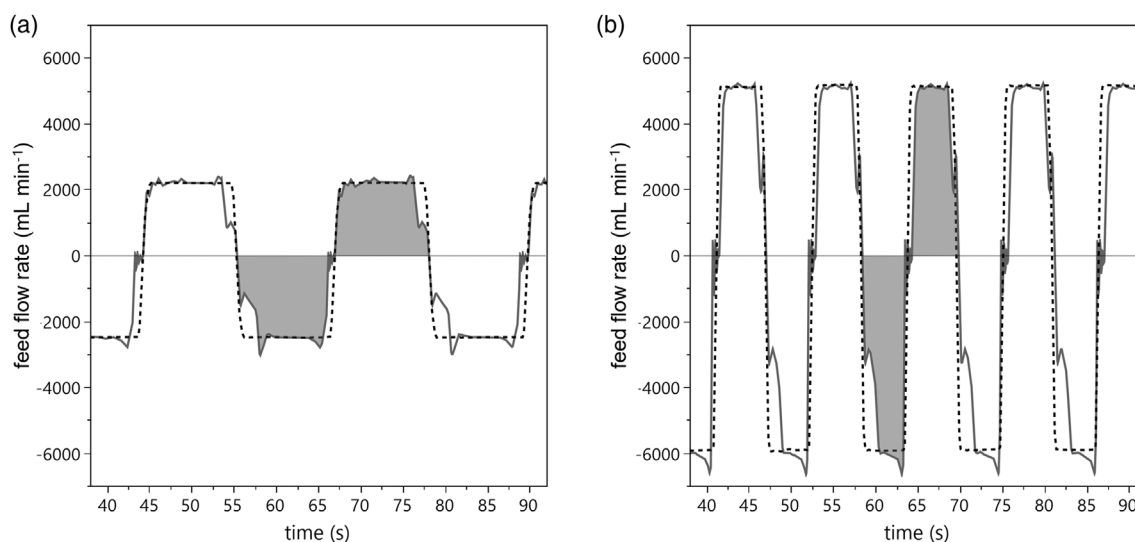


**FIGURE 2** Feed flow profiles of setup I (gray solid line) with feed flow rate set point of 2 L min<sup>-1</sup> (a) and 4 L min<sup>-1</sup> (b). The gray shaded area represents the displacement volume of the diaphragm pump, which is fixed at 400 ml. The flow profiles of setup I were reproduced with setup II (black dashed line)

crossflow filtration) with the same actual feed flow rate and permeate flow rate were conducted using only the inlet centrifugal pump of setup II, while the other centrifugal pump was set inactive and was flow-through by the retentate.

Prior to each filtration experiment, the module was flushed with desalted water and the pure water permeability was measured at 15°C. Afterwards, the water was removed from the vessel and the filtration setup. While setup II was fully drainable, setup I had some remaining water in the diaphragm pump, which was not drainable without disassembling, which will be important when discussing the measured dry matter contents. Subsequently, 8 L of the pre-cooled feed suspension was given to the tank, the stirrer was set to 150 rpm and one initial feed sample was drawn. Afterwards, the feed flow was started, followed by the permeate flow induced by peristaltic pumps. Each filtration experiment was conducted for 5 h, when possible. Filtration trials with a permeate to feed ratio of 1:5 could not be sustained for the time of 5 h, but had to be aborted earlier due to cell accumulation. For experiments with this extreme permeate to feed ratio, additional optimization trials with setup II were conducted, such as the adaption of phase duration to improve fluid exchange and the

use of flow control to overcome viscosity related flow reduction (see further details in the results Section 3.3). By using these harsh conditions, the system robustness and effect of optimization approaches can be assessed.

During filtration, flow and pressure data were logged and feed, retentate and permeate samples were drawn. It should be noted that by drawing samples from the retentate, accumulated cells were removed from the system, which is of relevance when evaluating cell accumulation. In addition, special attention was paid to the time of sampling, that is, to sample only during the forward phase as the feed and retentate composition differ between the two phases.

After use, the hollow fiber module was cleaned in a caustic and enzymatic cleaning step with 0.5% v/v Ultrasil 69 and 0.4% v/v Ultrasil 67 (Ecolab Deutschland GmbH, Monheim am Rhein, Germany) at 50°C for 40 min and evaluated for water permeability (>80% of first use permeability) before reuse. None of the runs reported was the first use run of the module. Therefore, the resulting water permeability values were all in a comparable range. Nonetheless, the runs presented in Table 1 were conducted in a randomized order. The optimization experiments were performed afterwards. Therefore, the

effect of the filter module lifetime on the presented results is expected to be minimal.

The time-resolved inline data for pressure and flow values were averaged in order to obtain data representing mean processing performance. The data processing was done according to Weinberger and Kulozik.<sup>30</sup> From these averaged flux ( $J$ ) and transmembrane pressure ( $\Delta p_{TM}$ ) data, the filtration resistance ( $R_{filtration}$ ) was calculated according to Equation (3), considering the permeate viscosity  $\eta$ . The permeate viscosity of some permeate samples was measured using a MCR302 rheometer (Anton Paar GmbH, Graz, Austria) equipped with a double gap geometry; it was similar to pure water viscosity.

$$J = \frac{\Delta p_{TM}}{R_{filtration} \cdot \eta} \quad (3)$$

All data collected during the filtration trials were evaluated and plotted using JMP<sup>®</sup> Pro 14.1.

### 3 | RESULTS AND DISCUSSION

#### 3.1 | Flow profile

In order to directly compare both setups, flow profiles from setup I were recorded and reproduced with setup II. Figure 2 shows the flow profiles for the two feed flow rates chosen for this study, 2 L min<sup>-1</sup> and 4 L min<sup>-1</sup> (set point of setup I, note that the actual flow rate in setup I was higher than the set point due to the indirect process control concept, measuring cycle times instead of flow rates). The resulting mean crossflow velocity was 0.05 to 0.06 m s<sup>-1</sup> for a set flow rate of 2 L min<sup>-1</sup> and 0.11 to 0.13 m s<sup>-1</sup> for a set flow rate of 4 L min<sup>-1</sup>, resulting in shear rates of approximately 500 s<sup>-1</sup> and 1000 s<sup>-1</sup>, respectively. It can be seen that the flow profile produced by the diaphragm pump of setup I was steep for both up- and downward flanks, but with minor peaks and fluctuations due to the technical nature of the diaphragm pump. These deviations from an ideal ramp-like flow profile were more pronounced at higher flow rates. Especially in the exhaust phase, the set flow rate could only be reached after a couple of seconds due to the inertia of vacuum generation. Therefore, deviation of the actual flow rate from the set flow rate was higher at higher flow rates and during the exhaust phase.

The flow profile produced by setup II followed an almost ideal saw-tooth-like flow profile. In other words, the flow profiles of both setups were not identical, but close enough to exclude an impact on the filtration performance per se and on the fouling mitigation effects of wall shear stress and flow reversal.

#### 3.2 | Comparative assessment of filtration performance

The filtration trials were conducted at different feed flow rates and different permeate flow rates according to Table 1. Figure 3 shows

process performance indicators of filtration trials conducted at equal feed flow rate but varying permeate flow rates (and thus varying permeate to feed ratio), while Figure 4 shows process performance indicators of filtration trials with equal permeate to feed ratio, but varying feed flow rates. This differentiation allows for the separate evaluation of the role of permeate to feed ratio on cell accumulation and of the crossflow velocity on fouling mitigation.

As can be seen from Figure 3, all filtration trials with a feed flow rate of 4 L min<sup>-1</sup> could be sustained for at least 5 h. The process performance was similar for both alternating setups I and II with only minor differences. For the filtration trial with conventional non-alternating crossflow, the process performance was worse than for the alternating crossflow conditions, as can be seen from an up to tenfold transmembrane pressure and filtration resistance developing over time, while also showing a considerably lower transmission of BSA (10 to 15% less than in setups I and II). This clearly shows the superior fouling mitigation effect of alternating crossflow during microfiltration as already described by Weinberger and Kulozik<sup>14</sup> for higher crossflow velocities (about 3 m s<sup>-1</sup> in comparison to 0.1 m s<sup>-1</sup> in this study).

In comparison to the major difference between conventional non-alternating and alternating crossflow filtration, the effects of varying permeate flow rates and the filtration setup were comparably small, but yet observable. Figure 3a shows that the transmembrane pressure was higher for trials with higher permeate flow rate. This increase of transmembrane pressure was proportional to the increase in permeate flow rate, since the difference between each pair of trials vanishes when considering the filtration resistance (see Figure 3b). The filtration resistance, however, reveals a minor difference between the two filtration setups, where the resistance using setup II was approximately 30% lower than for setup I. Also the pressure profiles, as exemplarily shown in Figure S2 for setup I and setup II, show only minor differences. The fluctuation of absolute pressures is stronger pronounced for setup I and all local pressures cyclically reach negative values due to the acting diaphragm pump. But the transmembrane pressure is slightly positive for both setups with only single outliers, which are probably just artifacts due to the high data acquisition rate. The lower fluctuation of pressures in setup II might be beneficial as it results in a more even transmembrane pressure distribution across the membrane module and better module usage.<sup>15</sup>

The BSA transmissions, as depicted in Figure 3c, for all alternating trials were comparable and scattered at about 100%. This high transmission value can be attributed to the rather large pore size of 0.5 μm and the overall low transmembrane pressure, which prevented an undesirable compaction of fouling material. The fact that BSA transmission values were partially above 100% might be due to analytical variations and possibly due to the approximation of the real transmission, by taking the feed BSA concentration and not the retentate BSA concentration inside the filtration device into account (see Equation (1)).

Lastly, the dry matter content in the retentate was determined as a measure for cell accumulation (see Figure 3d). Cell accumulation can be observed for both alternating flow setups. This is due to the hold-

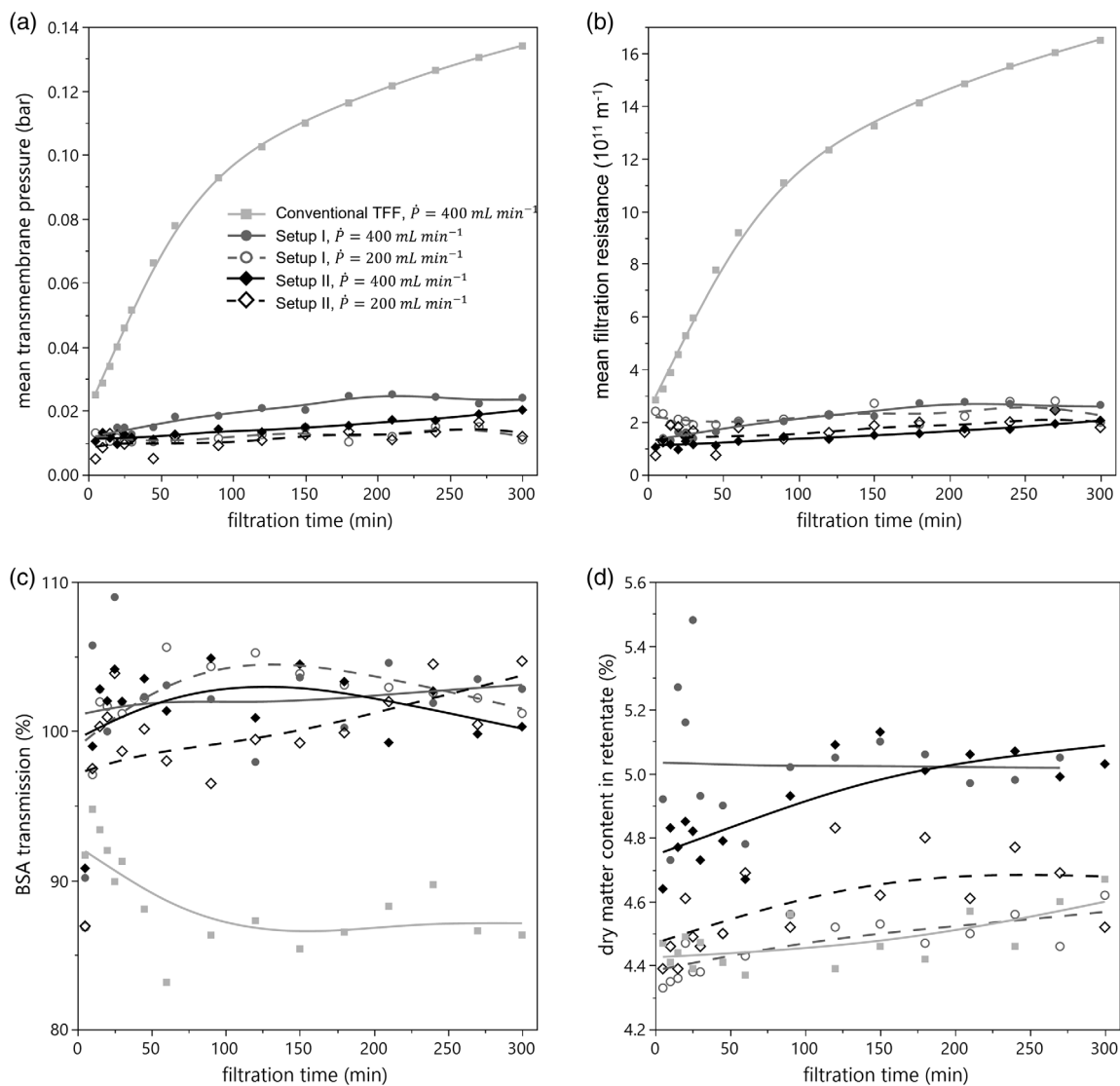


**FIGURE 3** Process performance indicators of filtration runs with a nominal crossflow of  $4 \text{ L min}^{-1}$ : (a) Transmembrane pressure, (b) filtration resistance, (c) BSA transmission, (d) dry matter content in the retentate. Dark gray circles refer to setup I, black diamonds to setup II and light gray squares represent a run with conventional non-alternating crossflow conducted with one centrifugal pump of setup II being active. Closed symbols with solid lines represent a permeate volume flow of  $400 \text{ ml min}^{-1}$  and open symbols with dashed lines of  $200 \text{ ml min}^{-1}$ . Lines are given as a guide to the eye.

up volume relative to the actual exchange volume ratio predetermined by setup I. The dry matter content in the retentate during conventional non-alternating crossflow filtration was, however, considerably lower than during alternating filtration, which indicates that the exchange volume of  $400 \text{ ml}$  was insufficient to reach a complete volume exchange in the hold-up volume of the filtration system ( $234 \text{ ml}$  in the hollow fiber retentate void volume plus tubing, equals approximately  $260 \text{ ml}$  for setup I and  $390 \text{ ml}$  for setup II). It can be seen that higher permeate to feed ratios ( $1:10$  in comparison to  $1:20$ ) led to higher dry matter contents with no significant difference between the two setups (where slightly lower dry matter content in setup I can be attributed to the incomplete draining after pure waterflux measurement, as explained in the methods section). This impact of the permeate to feed ratio is based on the concentration effect along the

membrane, which can be even more pronounced for alternating filtration systems, since each fluid element passes the membrane twice, considering incomplete fluid exchange.

The direct comparison of filtration trials with different feed flow rates, but a similar permeate to feed ratio of  $1:10$ , are presented in Figure 4. Data already shown in Figure 3 are included to allow for a direct comparison of the observed effects related to the impact of crossflow velocity on fouling mitigation, separately from cell accumulation effects. The transmembrane pressure was higher for trials with higher permeate flow rate and increased stronger over filtration time in comparison to trials with lower permeate flow rate, as depicted in Figure 4a. The filtration resistance, however, was lower for these trials (see Figure 4b). The lower filtration resistance can be attributed to the higher crossflow velocity, which enables an improved fouling

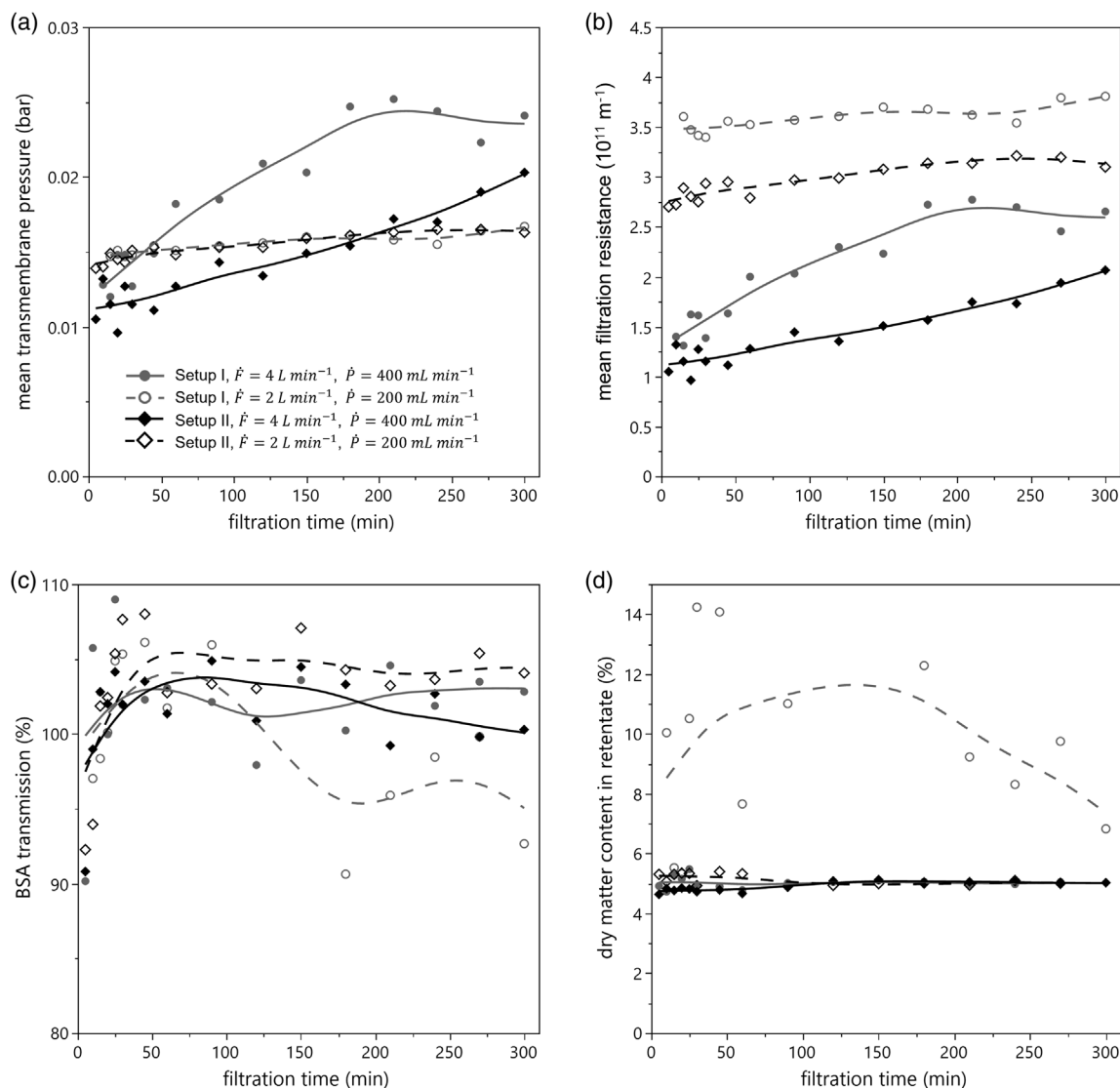


**FIGURE 4** Process performance indicators of filtration runs with a permeate to feed ratio of 1:10: (a) Transmembrane pressure, (b) filtration resistance, (c) BSA transmission, (d) dry matter content in the retentate. Dark gray circles refer to setup I, black diamonds to setup II. Closed symbols with solid lines represent a feed volume flow of  $4 \text{ L min}^{-1}$  and a permeate volume flow of  $400 \text{ mL min}^{-1}$  and open symbols with dashed lines of  $2 \text{ L min}^{-1}$  feed volume flow and  $200 \text{ mL min}^{-1}$  permeate volume flow. Lines are given as a guide to the eye.

mitigation due to higher wall shear stress. In addition, higher crossflow velocities are inextricably linked to a higher frequency of flow reversal in setup I, which also has a positive impact on fouling mitigation up to a limiting frequency.<sup>14</sup> This shows that the choice of crossflow velocity requires detailed experimental optimization when operating a perfusion device, which in our eyes is not sufficiently considered in many studies.

When comparing setup I and II, the filtration resistance in experiments using setup II was 20 to 30% lower than in experiments using setup I (as can be seen from Figure 4b), which is comparable to the observation from Figure 3b. The BSA transmission was not significantly different for most trials shown, with only a minor reduction after 3 h of filtration for the trial with  $2 \text{ L min}^{-1}$  feed flow rate conducted with setup I (gray open circles in Figure 4c). This trial also stands out in terms of accumulated dry matter in the retentate (see

Figure 4d). Whereas all other trials with a permeate to feed ratio of 1:10 showed similar dry matter contents in the retentate, the dry matter content in the retentate was approximately doubled for the  $2 \text{ L min}^{-1}$  trial conducted with setup I due to cell accumulation over time. Considering the difference between  $2 \text{ L min}^{-1}$  and  $4 \text{ L min}^{-1}$  feed flow rate, on the one hand, it seems that the lower feed flow rates resulted in drag forces too low to transport the easily sedimentable cells against gravity back into the feed tank. Considering the differences between the filtration setups, on the other hand, setup II has no dead-end, as it is characteristic for the diaphragm pump of setup I. Setup II thus draws fresh medium from the feed tank also during the backwards flow phase, which reduces or even avoids accumulation of cells during filtration even at low feed flow rates. Hence, it can be said that even when setup II was operated with similar flow profiles as setup I, which is unfavorable in terms of the insufficient exchange



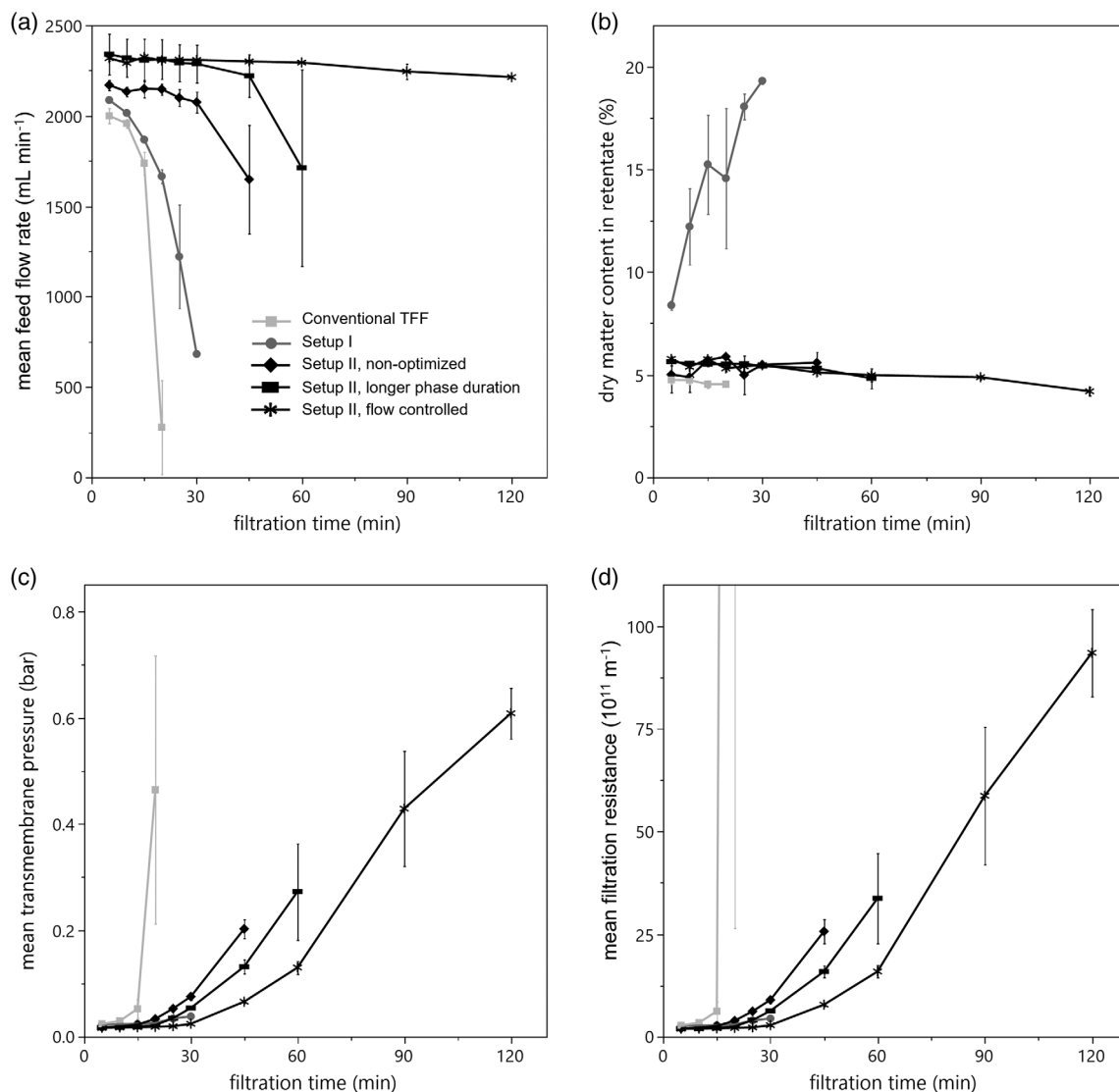


**FIGURE 5** Process performance indicators of filtration runs with a nominal crossflow of  $2 \text{ L min}^{-1}$  and a nominal permeate flow rate of  $400 \text{ ml min}^{-1}$ : (a) Actual mean feed flow rate, (b) dry matter content in the retentate, (c) mean transmembrane pressure, (d) mean filtration resistance. Dark gray circles refer to setup I, black diamonds setup II and light gray squares represent a run with conventional non-alternating crossflow conducted with one centrifugal pump of setup II being active. Black rectangles represent filtration trials with setup II, but prolonged forward and backwards phases and black asterisks represent filtration trials with setup II, where the pumps were flow controlled instead of speed controlled. The error bars indicate the range of a randomized duplicate. Lines are given as a guide to the eye

volume, the issue of cell accumulation was less severe and filtration resistances were thus reduced.

### 3.3 | Optimization concepts using setup II

Chapters 3.1 and 3.2 were based on process conditions defined by the feasible operating range of setup I. Setup II, however, is more flexible, since flow velocities and phase durations can be varied independently from each other. Two different process optimization concepts were tested based on the trial with the highest and extreme permeate to feed ratio (1:5) in order to make the differentiation and the future potential of the alternate flow concepts more obvious, that is,

$2 \text{ L min}^{-1}$  feed flow rate and  $400 \text{ ml min}^{-1}$  permeate flow rate. The first optimization concept takes advantage of the independence of feed flow rate and cycle time, which allows adapting the exchange volume. The second optimization concept is based on the automatic control of the feed flow, which allows counteracting increasing feed viscosity due to cell accumulation. For the sake of a direct comparison, results obtained with non-alternating crossflow conditions, setup I as well as the non-optimized setup II and the same permeate to feed ratio are given as well. For illustration, the flow profiles discussed in this chapter can be found in the supplementary information (Figure S1).

Figure 5 shows the process performance indicators for filtration trials conducted with  $2 \text{ L min}^{-1}$  feed flow rate and  $400 \text{ ml min}^{-1}$

permeate flow rate. It can be seen that, due to the deliberately chosen extreme permeate to feed ratio, none of the trials could be sustained for the filtration time of 5 hours. The high permeate rate led to the concentration of the retentate (see Figure 5b), which results in an increased retentate viscosity and an impaired pumpability. Note that the controller of setup I cannot satisfactorily cope with increased fluid viscosities.<sup>31</sup> As a result of cell accumulation and increased fluid viscosity, the feed flow decreases over time (see Figure 5a). The insufficient volume exchange in setup I and the non-optimized setup II, as discussed in chapter 3.2, aggravates this issue. Also, the high permeate to feed ratio, as intended, led to severe deposit formation, which can be concluded from increasing transmembrane pressures and filtration resistances (see Figure 5c,d).

During conventional non-alternating crossflow filtration, cell accumulation issues due to insufficient fluid exchange did not occur. However, the sharp increase of fouling resistance after 15 to 20 min of conventional non-alternating crossflow filtration at similar permeate to feed flow ratio (see Figure 5d), hints at severe deposit layer formation due to the high drag forces toward the membrane and insufficient fouling prevention. Obviously, alternating crossflow was able to mitigate fouling in an efficient way, resulting in a longer feasible filtration time of alternating crossflow for both setups I and II, despite the occurrence of cell accumulation. Therefore, an alternating flow filtration process, which efficiently mitigates fouling and avoids cell accumulation, increasing retentate viscosity and feed flow reduction (as occurring for setup I and non-optimized setup II) is desired.

In setup I, the exchange rate can only be increased by constructional means, such as a higher diaphragm pump volume (not in the operator's hands) or a shorter transfer line to the feed tank.<sup>27</sup> Using two counteractive centrifugal pumps in setup II, the fluid exchange can be easily improved by increasing the volume transported in each phase, that is, by increasing the phase duration (as shown in Figure S1C) and/or feed flow rate, or by counteracting the increasing retentate viscosity by implementing a feedback loop (as shown in Figure S1D). Both optimization options are addressed in the following.

By reducing cell accumulation, prolonged phases (compare phase duration from lower panels in Figure S1) not only led to a longer feasible filtration time, but also to a slower increase of the transmembrane pressure (Figure 5c). However, a slight decrease of the feed flow rate was nevertheless observed over time. Obviously, cell accumulation was not entirely prevented by prolonged, but still insufficiently long phases. In future, the optimum cycle times should be defined based on minimized hold-up volumes of the filtration loop, that is, long enough to support efficient fluid exchange and short enough to mitigate fouling by frequent flow reversal.

Controlling the feed flow rate instead of setting the pump speed to a predefined value helps to overcome the viscosity related feed flow reduction, where increasing pump speed compensates increasing fluid viscosities. In order to implement flow rate controlled alternating flow, quick responding pumps are essential and control parameters have to be optimized in order to reach steep ramps and avoid overshooting and oscillation. The flow profile reached with flow-controlled counteractive centrifugal pumps (setup II) is given in Figure S1D, lower panel. The

target flow rates and cycle times were chosen similar to the non-optimized setup II for comparability. The ramps were as steep as with a predefined pump speed (non-optimized setup II, see Figure S1B), while showing only minor overshoots and oscillations. From Figure 5a, it is evident that the feed flow rate did not decrease over time with the implemented feedback loop. However, the pump speed increases over time up to the maximum pump speed (data not shown) in order to compensate for the nonetheless increasing viscosity due to cell accumulation. Thus, the pumps used in this current setup eventually reached their final capacity (maximum revolution speed) and could no longer sustain the feed flow after 120 min. A sudden hollow fiber blockage and subsequent process abortion were the consequences. Besides the increased process time, fouling was reduced in comparison to the other trials with the same permeate to feed flow ratio, as can be seen from the lower filtration resistance (see Figure 5d).

Comparing all filtration trials at  $2 \text{ L min}^{-1}$  feed flow rate and  $400 \text{ ml min}^{-1}$  permeate flow rate, it becomes obvious that fouling was most severe for non-alternating conditions. By prolonging forward and backwards phase to ensure a complete hold-up volume exchange outside of the bioreactor (transfer lines, module volume) in each cycle and by implementing feed flow control in order to overcome viscosity related feed flow reduction, process times could be extended significantly.

The alternating flow profiles generated by the newly proposed system in this work were adjusted to flow profiles generated by the XCell ATF<sup>®</sup> for reasons of comparability and subsequently slightly adapted for optimization. Even these minor adaptations showed significant effects on process performance and robustness. It should, however, be noted that the concept of this newly proposed system allows to rethink alternating flow profiles and the optimization approaches shown in this work should only be seen as an indication of what could be further technically optimized:

- higher crossflow velocities and higher frequencies to increase fouling mitigation;
- higher crossflow velocities and longer phases to reduce cell accumulation at high permeate to feed ratios;
- longer forward phases with shorter intermittent backwards phases to combine the advantages of conventional and alternating crossflow;
- flow profiles with less steep ramps to protect shear-sensitive cells from turbulences;
- combination of alternating and pulsatile flow, where short flushing phases of higher flow rate might be used as inline cleaning technique.

However, these options are yet to be systematically investigated.

## 4 | CONCLUSION AND OUTLOOK

In this work, a new technical concept for alternating crossflow filtration was proposed and its hydrodynamic performance investigated in

direct comparison with the state-of-the-art XCell ATF<sup>®</sup> device and conventional non-alternating crossflow filtration.

Two counteractive centrifugal pumps instead of a single two-way diaphragm pump improved process performance in comparison to the XCell ATF<sup>®</sup> in terms of lower cell accumulation and lower filtration resistance. The fouling mitigation effect of alternating flow, formerly shown for high crossflow velocities and high transmembrane pressures, could be confirmed for low crossflow velocities and low transmembrane pressure conditions. This was done in a direct comparison with conventional non-alternating crossflow, without the additional impact of other circumstances, such as different shear forces for instance, as is the case for most direct TFF-ATF-comparisons. Based on the results presented in this work, the alternative design of alternating crossflow filtration concept could provide additional means to perform cell perfusion cultures under conditions less affected by membrane fouling and to longer sustainable cultivation before the membrane has to be replaced. The cell retention device proposed in this work was already successfully applied in mammalian perfusion cultures by project partners but discussing these results in detail would go beyond the scope of this work. Further technical optimization work could focus on a wider range of processing conditions and validation of effects for other cell systems can be considered based on the work presented here.

#### AUTHOR CONTRIBUTIONS

**Maria Weinberger:** Conceptualization (lead); data curation (lead); funding acquisition (lead); investigation (supporting); methodology (lead); project administration (lead); visualization (lead); writing – original draft (lead). **Luis Schoch:** Data curation (supporting); investigation (supporting); writing – review and editing (supporting). **Ulrich Kulozik:** Supervision (lead); writing – review and editing (lead).

#### ACKNOWLEDGMENTS

This work emerged from a bilateral research project between the Chair of Food and Bioprocess Engineering of the Technical University of Munich and Levitronix GmbH. The concept of two counteractive centrifugal pumps was proposed and implemented by Antony Sibilia from Levitronix GmbH. Also, the centrifugal pumps and online sensors used in this work were provided by Levitronix GmbH. We gratefully acknowledge the support from Levitronix GmbH as well as fruitful discussion with Antony Sibilia and Knut Kuss. Additionally, the authors want to thank F. X. Wieninger GmbH for the fresh baker's yeast supply. We acknowledge Hermine Rossgoderer and Heidi Wohlschläger from the Technical University of Munich for their analytical support in the HPLC laboratory. Open Access funding enabled and organized by Projekt DEAL.

#### CONFLICT OF INTEREST

The authors declare that they have no known competing financial interests or personal relationships that could have appeared to influence the work reported in this article. The counteractive centrifugal pump system was proposed and implemented by Antony Sibilia from Levitronix GmbH, the company selling magnetically levitating centrifugal pumps, which were presented as a core piece of equipment in the proposed filtration system. A patent application was filed for the

proposed filtration system, which is currently still pending. However, the findings in this work are based on experiments planned, conducted and interpreted by members of the Technical University of Munich. There was neither a consulting relationship nor honoraria paid to the members of Technical University of Munich by Levitronix GmbH. The experimental work did not receive financial funding from Levitronix GmbH or another third party.

#### DATA AVAILABILITY STATEMENT

The data that support the findings of this study are available from the corresponding author upon reasonable request.

#### ORCID

Maria E. Weinberger  <https://orcid.org/0000-0002-9781-7855>

#### REFERENCES

- Pollock J, Ho SV, Farid SS. Fed-batch and perfusion culture processes: economic, environmental, and operational feasibility under uncertainty. *Biotechnol Bioeng.* 2013;110(1):206-219.
- Warikoo V, Godawat R, Brower K, et al. Integrated continuous production of recombinant therapeutic proteins. *Biotechnol Bioeng.* 2012; 109(12):3018-3029.
- Walther J, Lu J, Hollenbach M, et al. Perfusion cell culture decreases process and product heterogeneity in a head-to-head comparison with fed-batch. *Biotechnol J.* 2019;14(2):1700733.
- Xu S, Gavin J, Jiang R, Chen H. Bioreactor productivity and media cost comparison for different intensified cell culture processes. *Biotechnol Prog.* 2017;33(4):867-878.
- Voisard D, Meuwly F, Ruffieux PA, Baer G, Kadouri A. Potential of cell retention techniques for large-scale high-density perfusion culture of suspended mammalian cells. *Biotechnol Bioeng.* 2003;82(7):751-765.
- Gränicher G, Coronel J, Trampler F, Jordan I, Genzel Y, Reichl U. Performance of an acoustic settler versus a hollow fiber-based ATF technology for influenza virus production in perfusion. *Appl Microbiol Biotechnol.* 2020;104(11):4877-4888.
- Karst DJ, Serra E, Villiger TK, Soos M, Morbidelli M. Characterization and comparison of ATF and TFF in stirred bioreactors for continuous mammalian cell culture processes. *Biochem Eng J.* 2016;110:17-26.
- Clincke M-F, Mölleryd C, Samani PK, et al. Very high density of Chinese hamster ovary cells in perfusion by alternating tangential flow or tangential flow filtration in WAVE bioreactor™—part II: applications for antibody production and cryopreservation. *Biotechnol Prog.* 2013;29(3):768-777.
- Karst DJ, Steinebach F, Soos M, Morbidelli M. Process performance and product quality in an integrated continuous antibody production process. *Biotechnol Bioeng.* 2017;114(2):298-307.
- Tapia F, Vázquez-Ramírez D, Genzel Y, Reichl U. Bioreactors for high cell density and continuous multi-stage cultivations: options for process intensification in cell culture-based viral vaccine production. *Appl Microbiol Biotechnol.* 2016;100(5):2121-2132.
- Padawer I, Ling WLW, Bai Y. Case study: an accelerated 8-day monoclonal antibody production process based on high seeding densities. *Biotechnol Prog.* 2013;29(3):829-832.
- Hadpe SR, Sharma AK, Mohite VV, Rathore AS. ATF for cell culture harvest clarification: mechanistic modelling and comparison with TFF. *J Chem Technol Biotechnol.* 2017;92(4):732-740.
- Wang S, Godfrey S, Ravikrishnan J, Lin H, Vogel J, Coffman J. Shear contributions to cell culture performance and product recovery in ATF and TFF perfusion systems. *J Biotechnol.* 2017;246:52-60.
- Weinberger ME, Kulozik U. On the effect of flow reversal during crossflow microfiltration of a cell and protein mixture. *Food Bioprod Process.* 2021;129:24-33.

15. Radoniqi F, Zhang H, Bardliving CL, Shamlou P, Coffman J. Computational fluid dynamic modeling of alternating tangential flow filtration for perfusion cell culture. *Biotechnol Bioeng.* 2018;115(11):2751-2759.
16. Weinberger ME, Kulozik U. Understanding the fouling mitigation mechanisms of alternating crossflow during cell-protein fractionation by microfiltration. *Food Bioprod Process.* 2022;131:136-143.
17. Hargrove S, Ilias S. Flux enhancement using flow reversal in ultrafiltration. *Sep Sci Technol.* 1999;34(6-7):1319-1331.
18. Hargrove SC, Parthasarathy H, Ilias S. Flux enhancement in cross-flow membrane filtration by flow reversal: a case study on ultrafiltration of BSA. *Sep Sci Technol.* 2003;38(12-13):3133-3144.
19. Hilal N, Ogunbiyi OO, Miles NJ, Nigmatullin R. Methods employed for control of fouling in MF and UF membranes: a comprehensive review. *Sep Sci Technol.* 2005;40(10):1957-2005.
20. Jaffrin MY. Hydrodynamic techniques to enhance membrane filtration. *Annu Rev Fluid Mech.* 2012;44(1):77-96.
21. Zhang W, Luo J, Ding L, Jaffrin MY. A review on flux decline control strategies in pressure-driven membrane processes. *Ind Eng Chem Res.* 2015;54(11):2843-2861.
22. Shevitz J. Fluid filtration system. US 6544424; 2003.
23. Shevitz J. Device, system and process for modification or concentration of cell-depleted fluid. US 10081788; 2018.
24. Pavlik R. Plunger pumping arrangement for a hollow fiber filter. US 2019/0201820 A1; 2019.
25. Pavlik R. Dual pumping arrangement for a hollow fiber filter. WO 2019/133487 A1; 2019.
26. Weinberger ME, Kulozik U. Pulsatile crossflow improves microfiltration fractionation of cells and proteins. *J Membr Sci.* 2021;629:119295.
27. Walther J, McLarty J, Johnson T. The effects of alternating tangential flow (ATF) residence time, hydrodynamic stress, and filtration flux on high-density perfusion cell culture. *Biotechnol Bioeng.* 2019;116(2):320-332.
28. Zhou H, Wright B, Yu M, Yin J, Konstantinov K. Methods and systems for processing a cell culture. EP3047013B1; 2014.
29. Kelly W, Scully J, Zhang D, et al. Understanding and modeling alternating tangential flow filtration for perfusion cell culture. *Biotechnol Prog.* 2014;30(6):1291-1300.
30. Weinberger ME, Kulozik U. Effect of low-frequency pulsatile cross-flow microfiltration on flux and protein transmission in milk protein fractionation. *Sep Sci Technol.* 2021;56(6):1112-1127.
31. Clincke M-F, Mölleryd C, Zhang Y, Lindskog E, Walsh K, Chotteau V. Very high density of CHO cells in perfusion by ATF or TFF in WAVE bioreactor™. Part I. Effect of the cell density on the process. *Biotechnol Prog.* 2013;29(3):754-767.

### SUPPORTING INFORMATION

Additional supporting information can be found online in the Supporting Information section at the end of this article.

**How to cite this article:** Weinberger ME, Schoch L, Kulozik U. New technical concept for alternating tangential flow filtration in biotechnological cell separation processes. *Biotechnol. Prog.* 2023;39(2):e3309. doi:[10.1002/btpr.3309](https://doi.org/10.1002/btpr.3309)